

DOI: 10.1002/sml.200600652

Compression-Modulated Tunable-Pore Carbon-Nanotube Membrane Filters***Xuesong Li, Guangyu Zhu, Jonathan S. Dordick, and Pulickel M. Ajayan**

In biological processes, precise control of the permeability of ions and molecules through the lipid membrane, which contains microporous pores and channels, is achieved through conformational change of the membrane proteins.^[1] Similar control over permeability is not attainable for general synthetic materials. The preparation of materials with different pore sizes has been enabled by altering the processing conditions, such as using a range of surfactants,^[2] choosing various template molecules,^[3] having different dip-coating cycles,^[4] and through varying temperatures^[5] and reaction times.^[6] Materials have also been fabricated that contain pores responsive to external stimuli, such as temperature and pH, and are, therefore, capable of changing permeability during operation. For example, poly(*N*-isopropylacrylamide) encapsulated in silica has an average pore size of 3 nm and exhibits a reversible on/off permeation behavior at the polymer transition temperature.^[7] In microfiltration, the flux through blends of poly(*N*-isopropylacrylamide) and poly(vinylidene fluoride) grafted with poly(acrylic acid) and poly(4-vinylpyridine) was simultaneously temperature- and pH-dependent.^[8] Although these stimuli-responsive materials are attractive, pore sizes cannot be preset for a specific separation target, nor can they be dynamically tuned during operation without changing the solution chemistry or temperature. A material whose pore size can be mechanically tuned would provide higher operational flexibility.

Carbon nanotubes engineered into various ordered architectures have many possible applications.^[9–13] Recently, it has been demonstrated that packed arrays of vertically aligned nanotubes can be used as membranes in mixture separation, either by directly utilizing the open-ended nanotubes^[14–16] or by using the interstitial spaces between nano-

tubes.^[17] In addition, our recent work showed that the vertically aligned multi-walled carbon-nanotube membranes (CNMs) are super-compressible^[18] and fully elastic, thus suggesting a unique possibility in membrane filtration in which the membranes can be made pore-tunable (reversibly) as they are mechanically compressed and released. This unique combination of properties of a nanotube membrane allows for the development of a filter that can be conveniently preset at different pore sizes, or used as a valve that can be preset to allow passage of select molecular species during a chemical or biochemical reaction. Here, using highly compressible tunable-pore nanotube membranes, we demonstrate the efficient filtration of a series of protein molecules with molecular weights ranging from 14 to 540 kDa (about 5–20 nm in size). Mixtures of proteins are also tested for separation efficiency by dynamically changing the compression applied to the membrane.

Figure 1 a and b shows schematically the structure of a CNM filter before and after applying mechanical compression to the membrane. Porous polymer films (PTFE with a pore size of 0.2 μm) were used to sandwich the nanotube membranes (3.5 mm in diameter), and act as a supporting base for applying compression to the whole filter assembly. The carbon nanotubes (Figure 1 c and d) were synthesized by the injection chemical vapor deposition (CVD) method reported previously.^[19] We have recently shown that aligned nanotube films exhibit super-compressive behavior,^[18] undergo fully elastic compression up to 15% of the original film thickness, and are fully resilient upon load release. During compression cycles, the nanotubes collectively form zigzag buckles,^[18] reversibly and fully reconfiguring the interstitial spaces (Figure 1 e). Since the nanotube films do not expand laterally on compression, the volume change transfers into pore size change, which is reversible upon compression and release. Thus, the permeability of the CNM can be tuned by adjusting the compression level, as demonstrated by the flux of water as a function of pressure drop and CNM compression (Figure 1 f). The inset in Figure 1 f also suggests that at low compressions (< 40%) permeability is more sensitive to compression changes than at higher compressions.

This unique tunable-pore property of the nanotube membrane allows us to perform the separation of species of different sizes, within the expandable pore-size range in the nanotube membrane, without changing the filter but simply by setting the same membrane at different thicknesses via uniaxial compression. This property also makes the CNM ideal for the early-stage size-selective separation of particle mixtures, such as those of biological macromolecules.

To test the tunability of the CNM, we performed unstirred dead-end filtration of a series of proteins, including lysozyme, α -chymotrypsin (α -CT), superoxide dismutase, α -amylase, glucose oxidase, and β -galactosidase, with molecular weights ranging from 14 to 540 kDa which correspond to sizes ranging from approximately 5 to 20 nm (Table S1, Supporting Information). Protein solutions were prepared in ultrapure water and the concentrations of the original solution and the filtrate were measured spectrophotometrically at 280 nm. The observed retention f was calculated by the

[*] X. Li, Prof. P. M. Ajayan
Department of Materials Science & Engineering
Rensselaer Polytechnic Institute
Troy, NY 12180 (USA)
Fax: (+1) 518-276-8554
E-mail: Ajayan@rpi.edu

Dr. G. Zhu, Prof. J. S. Dordick
Department of Chemical & Biological Engineering
Rensselaer Polytechnic Institute
Troy, NY 12180 (USA)

[**] This work was supported by an NSF-NSEC grant (DMR-0117792). The authors also acknowledge Dr. Anyuan Cao for providing the SEM image of the compressed CNM.

Supporting information for this article is available on the WWW under <http://www.small-journal.com> or from the author.

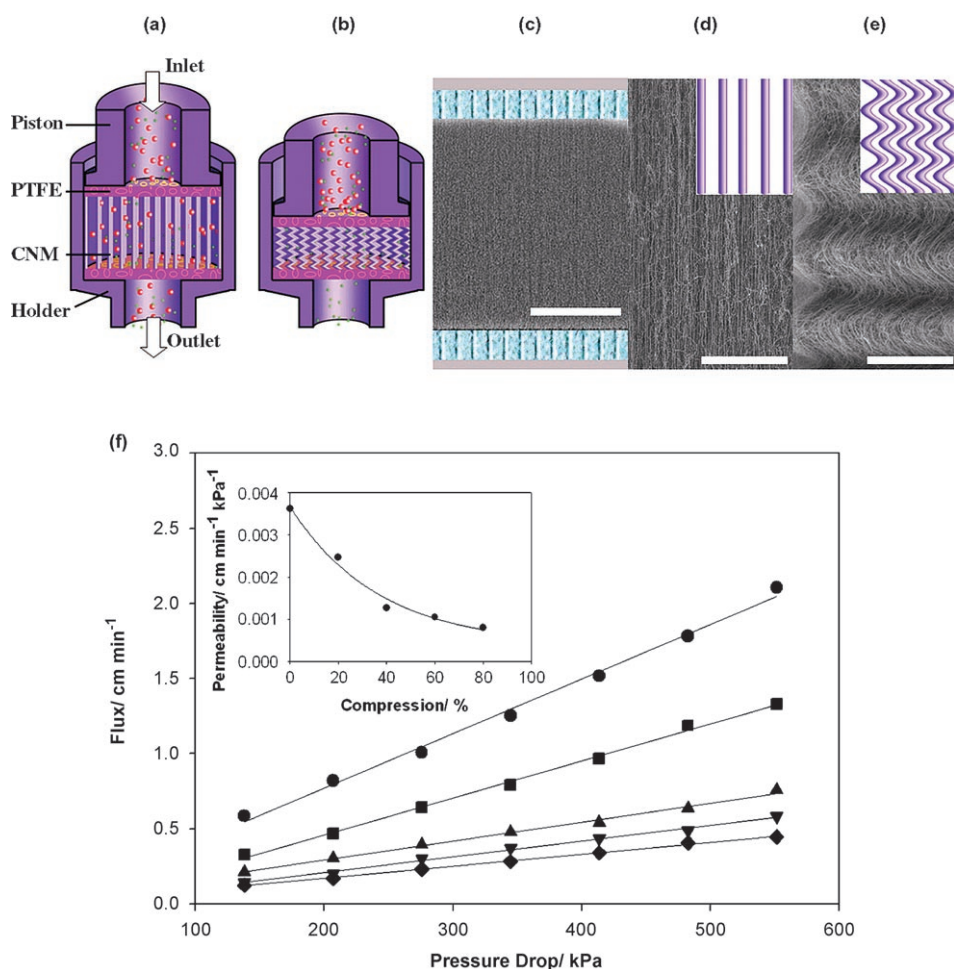


Figure 1. a, b) Schematics of the tunable CNM filter, c–e) scanning electron microscopy (SEM) images of an uncompressed and compressed CNM, and f) the permeability change of the CNM at different compressions. Porous PTFE films with a pore size of 0.2 μm are used to support the CNM. The piston is mounted on a nut and can move back and forth to compress/release the CNM. a) Without compression, both large and small particles can pass through the filter; b) at a certain compression larger particles are retained due to reduced internanotube distance/pore size; c, d) SEM images of the straight, uncompressed CNM at low and high magnifications, respectively; e) SEM image of the CNM under compression. The insets in (d) and (e) schematically depict the influence of compression on change in pore size. f) The solvent (water) flux change as a function of pressure drop for the CNM under different compressions: \bullet 0, \blacksquare 20, \blacktriangle 40, \blacktriangledown 60, and \blacklozenge 80%. The inset in (f) is the permeability (which is given by the slope of the curves in (f)) of the CNM as a function of compression. Scale bars: 100 μm for (c); 10 μm for (d) and (e). To denote the degree of compression we use the expression $(1 - \frac{\text{thickness under compression}}{\text{original thickness}})$; that is, 0% means no compression and 80% indicates the CNM is compressed to 20% of its original thickness.

formula $f = [(C_i - C_f)/C_i] \times 100\%$, where C_i is the initial concentration before filtration and C_f is the concentration of the filtrate. Filtration of these proteins by the PTFE film (0.2 μm pore size) without CNM showed no retention.

Proteins may adsorb onto the carbon-nanotube surface due to hydrophobic interactions,^[20] thus causing a higher observed retention for the freshly prepared CNM filter. This is shown in Figure S1 (Supporting Information) for α -CT through a CNM filter with 0, 20, and 60% compression. After protein adsorption reaches equilibrium (about five to six filtration cycles, with each cycle generating 0.6 mL of filtrate), the observed retentions are mainly due to pore rejection. We used α -CT (20%) to passivate the CNM mem-

branes, because of its relatively small size and demonstrated complete inactivation upon being adsorbed onto carbon nanotubes, and then determined the effect of CNM compression on filter permeability by filtration of different proteins.

The influence of CNM compression on the filtration of various protein solutions (concentration $\approx 16 \mu\text{M}$) is depicted in Figure 2a. The retention of larger proteins is more significantly impacted by compression than that of smaller proteins. The retention of smaller proteins (e.g., α -CT, lysozyme, and superoxide dismutase) is linearly related to CNM compression before the proteins are fully retained, which indicates that the pore size distribution changes monotonically upon CNM compression. For large proteins ($> 160 \text{ kDa}$), 99% retention is achieved at 40% compression of the CNM, while for intermediate-size proteins ($\approx 50 \text{ kDa}$) a similar retention requires about 60% compression. For small proteins ($< 35 \text{ kDa}$), nearly complete retention (i.e., 99%) cannot be achieved even at 80% compression.

The influence of protein molecular weight on retention is more directly seen in Figure 2b. The highest selectivity is observed in the compression range of 20–60%. Interestingly, the retention appears to show anomalous

behavior for lysozyme ($\log M_r = 4.15$; M_r = relative molecular mass), which appears to be retained more easily than its molecular weight would predict. Although lysozyme is highly positively charged, its filtration at high pH and high ionic strength did not show decreased retention (Figure S2, Supporting Information), which suggests that this anomalous behavior was not due to electrostatic interactions. However, this behavior may be rationalized by understanding the separation behavior of proteins that are not uniformly globular. In the case of lysozyme, the characteristic dimensions are $7.9 \times 7.9 \times 3.8 \text{ nm}^3$; hence, one of the dimensions is far shorter than the other two, perhaps aiding anisotropic tumbling through the CNM pores. Similar anisotropy would

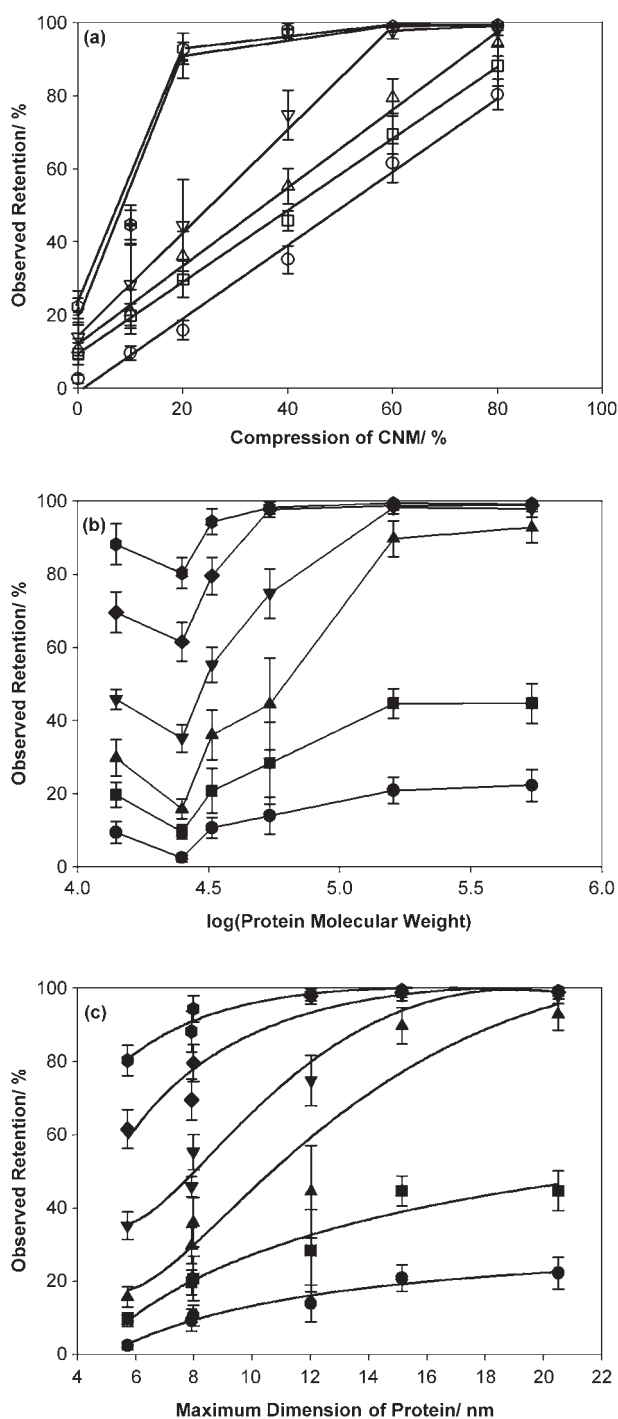


Figure 2. Size-selective properties of the CNM filter as a function of compression. a) Observed retention of different proteins versus compression of CNM. ○: α -chymotrypsin, □: lysozyme, △: superoxide dismutase, ▽: α -amylase, +: glucose oxidase, ⊗: β -galactosidase. b) Protein size as reflected by $\log M$, values at different compression levels and c) protein size as reflected by maximum length dimension at different compression levels. For (b) and (c) compression: ● 0, ■ 10, ▲ 20, ▼ 40, ◆ 60, ⊗ 80%. All protein concentrations were $16 \mu\text{M}$, and the data were obtained from three different membranes and averaged.

be expected for other proteins, for example, α -amylase and glucose oxidase; however, they are substantially retained by the CNM and the deviation in Figure 2b is less apparent. When we plot observed retention as a function of the maximum dimension of the protein (Figure 2c), which takes into account the most critical parameters involved in filtration, these size effects become more evident.

To evaluate the effect of sample-to-sample variation of the CNM on filtration (in Figure 2 all data were averaged over three different membranes), we further conducted filtration through five different CNM membranes at 20 and 60% compression (see Figure 3). These membranes were

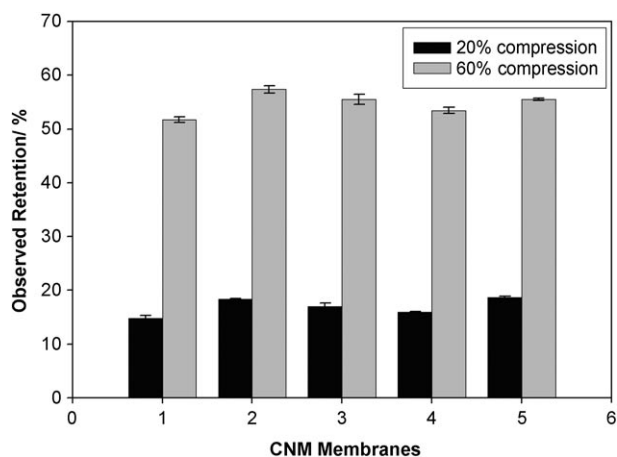


Figure 3. Filtration of an α -CT solution ($16 \mu\text{M}$) through five separately prepared membranes. The first four membranes were as-grown, while membrane 5 was pretreated by 200 sequential compression–release cycles at the maximum compression of 80% before being used for filtration.

synthesized in different batches but under the same process conditions. Membrane 5 was “pretreated” by undergoing 200 sequential compression–release cycles at the maximum compression of 80% before being used for filtration. The high consistency of performance of these membranes indicated that they have very similar pore characteristics.

To exploit the selectivity of the CNM, we examined the separation of a mixture containing a variety of proteins, including lysozyme, superoxide dismutase, trypsin, alcohol dehydrogenase, α -amylase, β -glucosidase, and bovine serum albumin (BSA; each individual protein at a concentration of 0.25 mg mL^{-1}), at sequentially increased compression levels. Qualitative analysis of the resulting filtrates was performed by sodium dodecyl sulfate polyacrylamide gel electrophoresis (SDS-PAGE). As expected, high retention of large proteins was achieved at about 40% compression (Figure S3, Supporting Information). Filtration through the CNM did not lead to enzyme deactivation—activity tests (with the exception of the nonenzymatic BSA) showed no loss of specific enzymatic activity after filtration, thus indicating full preservation of the native protein function. Therefore, use of the CNM filters offers a promising approach to the facile and rapid separation of biological molecules.

The mechanical response of the CNM in compression exhibits excellent resilience and the filter can be elastically cycled hundreds of times without any significant reduction in the CNM thickness.^[18] This provides an easy way to clean the membranes. After being released, the original internanotube distances (hence the pore sizes) recover and the particles entrapped in the membrane can be easily flushed out. Our experiments show that after the compressed CNMs were released and washed several times with water, no protein was found in the filtrate.

The CNM can also function as an enzyme reactor, as shown schematically in Figure 4. This simple device com-

Substrate conversions of 17 and 60% were obtained for 0 and 40% compression, respectively (Figure 4d), which indicates effective retention of the enzyme within the CNM and its resulting catalytic activity. The activity of the enzyme entrapped in the 40% compressed CNM was measured as $0.19 (\mu\text{mol product})(\text{mg enzyme})^{-1}\text{s}^{-1}$. In comparison, the solution-phase activity was $0.21 (\mu\text{mol product})(\text{mg enzyme})^{-1}\text{s}^{-1}$; hence, the β -galactosidase within the CNM retained its native activity. It may be imagined that the enzyme loading can be readily adjusted by changing the compression on the CNM and the concentration of the enzyme solution without affecting the permeability of the products, which are much smaller than the enzyme.

In conclusion, we have demonstrated the tunable porosity property of CNMs simply by applying different levels of compression. These CNMs can also act as immobilized enzyme reactors, which can lead to facile, integrated, and continuous-flow biotransformation–separation systems. The concept of a pore-size-changing membrane may be found in biological systems, such as the glomerular basement membrane in the kidney, in which the membrane permeability changes due to membrane compression caused by applied pressure.^[21] In addition, the concept may have potential in the development of artificial biomedical devices, such as in the construction of membranes and cartilages incorporating enzymes to remove toxins from blood and other bodily fluids, thus adding new dimensions to synthetic biomimetic design.^[22]

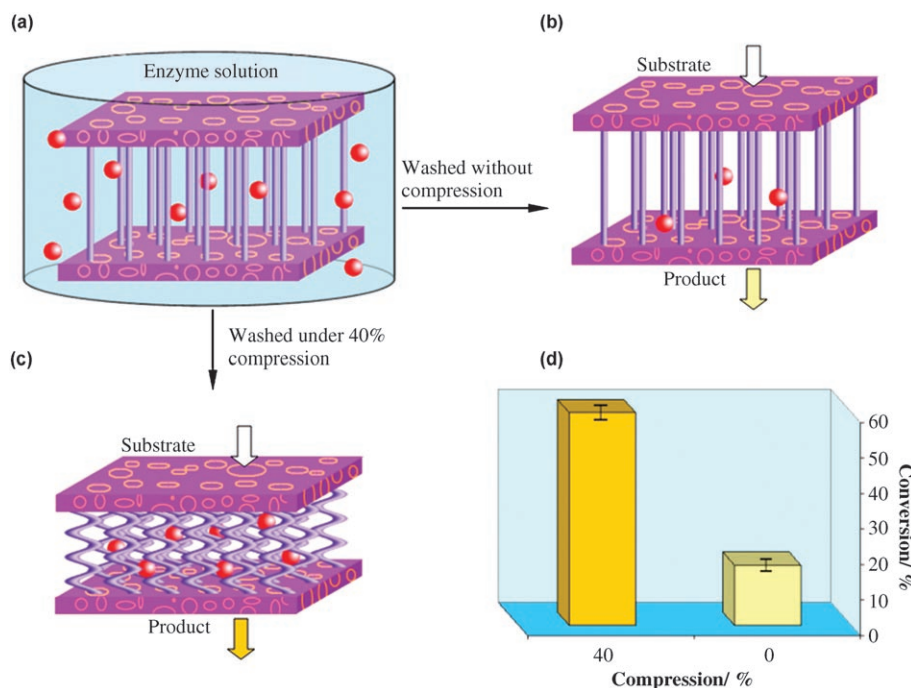


Figure 4. Schematic of the CNM as an entrapped β -galactosidase reactor. a) Enzyme solution was initially passed through the uncompressed CNM. b) The CNM at zero compression was washed with buffer and then substrate solution was passed through the membrane. A small fraction of enzyme molecules (indicated as red balls) was retained by nonselective adsorption and entrapment. c) The CNM at 40% compression was washed with buffer and then substrate solution was passed through the membrane. When compared to (b), a larger amount of enzyme was entrapped in the CNM due to the decreased pore size. d) Substrate conversions of 60 and 17% were obtained at 40 and 0% compression of the CNM, respectively.

bines easy enzyme immobilization and biocatalytic transformation with product separation. To demonstrate this concept, we chose β -galactosidase as a model enzyme for its ability to catalyze the hydrolysis of simple sugar derivatives, such as *o*-nitrophenyl- β -D-galactopyranoside (ONPG). The enzyme solution was passed through an uncompressed CNM (Figure 4a), and then the CNM was set at 0% (Figure 4b) or 40% (Figure 4c) compression and washed with buffer to remove free and loosely bound enzyme molecules until no enzyme was detected in the respective filtrates. The substrate solution (ONPG) was then passed through the CNMs with the same flux and the *o*-nitrophenol product in the filtrates was detected spectrophotometrically at 405 nm.

Experimental Section

CNM preparation: The CNM was fabricated by catalytic CVD. An Ar/H₂ mixture (85:15 vol%) was used to flush out air in the reaction chamber, and a solution of xylene and ferrocene (100 mL; 1 g) was injected into the first heating stage (steel chamber) by a syringe pump at a rate of 0.11 mL min^{-1} and vaporized at 180°C . The vapor was carried by Ar/H₂ at a flow rate of $100 \text{ cm}^3 \text{ min}^{-1}$ into the second heating stage (tube furnace) preheated to 770°C . The CNM, made up of uniformly spaced, aligned arrays of multi-walled carbon nanotubes, was then grown on a SiO₂ substrate placed at the center of the furnace tube and was peeled off from the substrate with relative ease.

The thickness of nanotube membrane grown in 30 min was about 300 μm . The average diameter of the nanotubes was 30 nm (Figure S4, Supporting Information). The bulk density (mass divided by the whole volume) of the CNM was 0.07 g cm^{-3} .

Filtration of protein solution: In the multi-walled nanotube membranes used here, the flow occurs essentially via the interstitial spaces between individual tubes and not through the pores within the tubes, as the ends of the tubes are unopened. Although there is a distribution of diameters for the nanotubes in the membrane (Figure S5, Supporting Information), the interstitial pore size distribution falls within the range of 10–34 nm.^[23]

All experiments were performed as unstirred dead-end filtration through a CNM with a diameter of 3.5 mm and original thickness of 300 μm . Pressure was applied by a helium gas cylinder and controlled by a gas regulator. Protein solutions were prepared by dissolving lysozyme, α -CT, superoxide dismutase, α -amylase, glucose oxidase, or β -galactosidase in ultrapure water to a final concentration of 16 μM . The α -CT solution was first passed through the CNM until equilibrium protein adsorption was achieved. The protein solutions (0.6 mL) were then passed through the CNM set at different compression levels and the protein concentrations of the filtrates were measured using a UV/Vis spectrophotometer (Shimadzu UV-2401) at 280 nm. Between each measurement the compressed membrane was released and washed with ultrapure water.

CNM enzyme reactor: β -Galactosidase was dissolved in phosphate buffer (0.05 M, pH 7.0) to make a final concentration of 0.7 mg mL^{-1} . The enzyme solution was used to soak the un-compressed CNM and then zero or 40% compression was applied to the CNM. A specific amount of enzyme was spatially entrapped in the CNM membrane in addition to that which adsorbed onto the nanotubes. Only strongly adsorbed and spatially confined enzymes were held in the CNM membrane after washing with buffer (phosphate, 0.05 M, pH 7.0). The amount of enzyme in the zero and 40% compressed CNM was measured to be approximately 0.03 and 0.11 mg, respectively. The substrate solution (0.16 mM *o*-nitrophenyl- β -D-galactopyranoside dissolved in phosphate buffer) was then passed through the CNMs at a flow rate of 0.5 $\text{mL min}^{-1} \text{cm}^{-2}$ and the absorbance of the filtrate (0.6 mL) was measured at 405 nm to determine the *o*-nitrophenol product generated. The enzyme activity was expressed as ($\mu\text{mol product generated}(\text{mg enzyme})^{-1} \text{s}^{-1}$).

Keywords:

carbon nanotubes • filters • membranes • proteins

- [1] R. B. Gennis, *Biomembranes: Molecular Structure and Function*, Springer, **1989**.
- [2] X. Wang, J. Ma, J. Liu, C. Zhou, Y. Zhao, S. Yi, Z. Yang, *Nanotechnology* **2006**, *17*, 3627–3631.
- [3] Y. Shin, J. Liu, L. Q. Wang, Z. Nie, W. D. Samuels, G. E. Fryxell, G. J. Exarhos, *Angew. Chem.* **2000**, *112*, 2814–2819; *Angew. Chem. Int. Ed.* **2000**, *39*, 2702–2707.
- [4] S. Yoo, D. M. Ford, D. F. Shantz, *Langmuir* **2006**, *22*, 1839–1845.
- [5] Y. Tang, A. Li, D. Wu, Y. Chen, *Nanotechnology* **2006**, *17*, 2023–2026.
- [6] N. Singh, S. M. Husson, B. Zdyrko, I. Luzinov, *J. Membr. Sci.* **2005**, *262*, 81–90.
- [7] G. V. R. Rao, M. E. Krug, S. Balamurugan, H. Xu, Q. Xu, G. P. Lopez, *Chem. Mater.* **2002**, *14*, 5075–5080.
- [8] G.-Q. Zhai, Y. Lei, E. T. Kang, K. G. Neoh, *Surf. Interface Anal.* **2004**, *36*, 1048–1051.
- [9] R. H. Baughman, A. A. Zakhidov, W. A. de Heer, *Science* **2002**, *297*, 787–792.
- [10] W. A. de Heer, W. S. Bacsá, A. Châtelain, T. Gerfin, R. Humphrey-Baker, L. Forro, D. Ugarte, *Science* **1995**, *268*, 845–847.
- [11] K. Jiang, Q. Li, S. Fan, *Nature* **2002**, *419*, 801.
- [12] A. Modi, N. Koratkar, E. Lass, B. Q. Wei, P. M. Ajayan, *Nature* **2003**, *424*, 171–174.
- [13] M. Zhang, S. L. Fang, A. A. Zakhidov, S. B. Lee, A. E. Aliev, C. D. Williams, K. R. Atkinson, R. H. Baughman, *Science* **2005**, *309*, 1215–1219.
- [14] S. A. Mille, V. Y. Young, C. R. Martin, *J. Am. Chem. Soc.* **2001**, *123*, 12335–12342.
- [15] B. J. Hinds, N. Chopra, T. Rantell, R. Andrews, V. Gavalas, L. G. Bachas, *Science* **2004**, *303*, 62–65.
- [16] J. K. Holt, H. G. Park, Y. M. Wang, M. Stadermann, A. B. Artyukhin, C. P. Grigoropoulos, A. Noy, O. Bakajin, *Science* **2006**, *312*, 1034–1037.
- [17] A. Srivastava, O. N. Srivastava, S. Talapatra, R. Vajtai, P. M. Ajayan, *Nat. Mater.* **2004**, *3*, 610–614.
- [18] A. Y. Cao, P. L. Dickrell, W. G. Sawyer, M. N. Ghasemi-Nejhad, P. M. Ajayan, *Science* **2005**, *310*, 1307–1310.
- [19] B. Q. Wei, R. Vajtai, Y. Jung, J. Ward, R. Zhang, G. Ramanath, P. M. Ajayan, *Nature* **2002**, *416*, 495–496.
- [20] S. S. Karajanagi, A. A. Vertegel, R. S. Kane, J. S. Dordick, *Langmuir* **2004**, *20*, 11594–11599.
- [21] K. Klaentschi, J. A. Brown, P. G. Niblett, A. C. Shore, J. E. Tooke, *Am. J. Physiol.* **1998**, *274*, H1327–H1334.
- [22] R. Langer, D. A. Tirrell, *Nature* **2004**, *428*, 487–492.
- [23] J. T. Drotar, B. Q. Wei, Y. P. Zhao, G. Ramanath, P. M. Ajayan, T. M. Lu, G. C. Wang, *Phys. Rev. B* **2001**, *64*, 125417-1–125417-6.

Received: November 20, 2006

Published online on ■ ■ ■ ■, 2007

Membrane filters

X. Li, G. Zhu, J. S. Dordick,

P. M. Ajayan* ————— ■■■■ — ■■■■

Compression-Modulated Tunable-Pore Carbon-Nanotube Membrane Filters

Turn on the pressure: Vertically aligned carbon-nanotube membranes show super-compressive and elastic properties. The pore size can be dynamically and reversibly controlled by mechanical deformation of the membrane, over ranges useful for ultrafiltration (see picture). The separation of proteins with molecular weights of 14–540 kDa (about 5–20 nm in size) is demonstrated with a single membrane set at different pore sizes by mechanical stress.

